J MATER RES TECHNOL. 2019;xxx(xx):xxx–xxx

Available online at www.sciencedirect.com

jmr&t Journal of Materials Research and Technology

www.jmrt.com.br

Original Article

Variation in mechanical properties with MnO_2 content in cast and forged in-situ Al-8Mg-MnO_2 composites

Vikas Narain[a,*], *Subrata Ray*[b]

[a] *Shri Bhawani Niketan Insititute of Technology and Management, Jaipur, India*
[b] *Indian Institute of Technology Mandi, India*

ARTICLE INFO

Article history:
Received 10 November 2017
Accepted 27 July 2019
Available online xxx

Keywords:
Fracture toughness
Al-Mg-MnO_2 composite
J_{IC}
Mechanical properties
Growth toughness
Forged

ABSTRACT

Particulate Al-8Mg-MnO_2 composite is synthesized using stir cast method by adding 3, 5 and 8 wt% of MnO_2 powder in Al-8Mg melt and subsequently hot forged at 400 °C. It shows intermetallic precipitates containing Al, Mg and Mn at dendrite boundaries and embedded alumina and MnO_2 particles in the matrix. A significant improvement in hardness is observed as the percentage of MnO_2 particles increases from 3 to 8%. Similar trend is noticed in the forged samples. An increase in tensile and yield strength is also there as the percentage of MnO_2 increases in cast composite. Forging has enhanced the yield and tensile strength further keeping the trend similar to that of as cast composite. Increase in MnO_2 percentage has adverse impact on percentage elongation. Forged samples also show a similar trend of decrease in percentage elongation. Whereas forging has improved the initial fracture toughness J_{IC}. There is a decrease in J_{IC} when the percentage of particles increases in both the cast and the forged composites. 3 wt% MnO_2 in composite gives significant advantage in growth toughness without impairing initiation fracture toughness over that of the alloy. Increase in particle addition beyond 3 wt% of MnO_2 decreases both the initiation fracture toughness and the growth toughness rapidly.

1. Introduction

Metal matrix composites (MMCs) specially Aluminium alloy based composites are very attractive on account of their higher elastic modulus and strength to weight ratio, which makes them attractive for making light weight components in automobiles and aircrafts industry [1,2]. *In-situ* Al alloy-Al_2O_3 composites have been synthesized with variety of externally added metal oxides which get reduced by molten aluminum to generate alumina particles and releases useful alloying elements in the remaining molten aluminum. TiO_2 [3], MnO_2 [4], SiO_2 [5], CuO [6,7], B_2O_3 [8], MoO_3 [9], ZnO [10], and Fe_2O_3 [11] are used to produce in-situ composites. Hamid et al. [12] developed Al(Mg,Mn)-Al_2O_3 (MnO_2) composites by dispersion of MnO_2 particles in Al-Mg melt and reaction released manganese in the melt, which results in nucleation of $MnAl_6$ and alumina in the matrix. The composite shows increased strength in comparison to that of base alloy without affecting much of its ductility. Effect of different molds on ductility were studied by Shabestari and Moemeni [13] who found that

* *Corresponding author.*
E-mail: vikasnarain@yahoo.com (V. Narain).
https://doi.org/10.1016/j.jmrt.2019.07.062

Please cite this article in press as: Narain V, Ray S. Variation in mechanical properties with MnO_2 content in cast and forged in-situ Al-8Mg-MnO_2 composites. J Mater Res Technol. 2019. https://doi.org/10.1016/j.jmrt.2019.07.062

the graphite mold produces higher ductility out of four different types of molds made of graphite, copper, cast iron, and sand. Caceres et al. [14] and Wang [15] observed that higher solidification rates lead to the largest elongation. On the other hand Mae et al. [16] found low solidification rate had higher yield strength and lower ductility. It means solidification rate has critical impact on mechanical properties of the composite. Zhang et al. [17] had prepared Al–$Zr(CO_3)_2$ composites by adding different amounts of $Zr(CO_3)_2$ (5, 10, 15, 20, and 25 wt%) particles at 900 °C, which had generated in-situ particles of Al_2O_3 and Al_3Zr in the melt. They found that the tensile and yield strengths of the in-situ composites were much higher than those of pure aluminum and increases with increasing wt% of $Zr(CO_3)_2$. Xing et al. [18] had studied Ni-Al based composite reinforced with 0–20 vol% of TiC particles and observed that yield strength of hot pressed composite was three times higher than that of the matrix at 980 °C. The fracture toughness was also 50% higher than that of the matrix. It suggests that hot pressing has impact on yield strength as well as on fracture toughness. Manoharan and Lewandowski [19] had studied crack initiation and growth toughness in Al-Zn-Mg-Cu alloy containing 0, 15, 20% by volume of SiC and observed that both the fracture initiation J_{IC} and growth toughness were similar to that of the un-reinforced and over-aged un-reinforced conditions. The fracture initiation toughness, J_{IC}, and crack growth toughness of the under-aged composite was about twice that of the over-aged composite reinforced with 5 μm SiC as well as with 13 μm SiC [20]. The under-aged composite exhibited a linear decrease in J_{IC} as the volume fraction of SiC increases in the range 0–20% while the over-aged composite exhibited a more rapid decrease in J_{IC} over the same range of volume fractions. However, J_{IC}, shows only a minor dependence on the size of the reinforcement [19]. The crack growth toughness is usually assessed in terms of the slope of the *J-R* curve which is evaluated in terms of the non-dimensional tearing modulus, T_R, [20] as

$$T_R = \frac{E}{\sigma_f^2}\frac{dJ}{da} \quad (1)$$

Where, E is the elastic modulus, σ_f is the flow stress and $\frac{dJ}{da}$ is the slope of the *J-R* curve. The slope of the linear segment of the valid points on the *J-R* curve is divided by the square of flow stress to determine T/E ratio. Extrusion, rolling, forging etc are the processes which have been used to eliminate the casting defects like porosity, voids and others. Extruded aluminium-SiC composite improves the yield and tensile strength by 40% in comparison to that of as cast composite [21]. The extruded samples demonstrate better ductility because of reduction in reinforcement particle size, absence of particle de-cohesion, and the improvement of particle-matrix interfacial bond. Pillai et al. [22] have observed that at a given vol% of graphite, the forged composites show higher toughness than those of cast composites. Balasubramaniam et al. [23] noted that forging had opened up TiO_2 particles clusters in Al-Zn-Mg alloy based composite, which resulted into voids and deteriorated mechanical properties. Ghanaraja et al. [24] observed that higher addition of nano sized MnO_2 powder results in deterioration of mechanical properties, possibly due to clustering and porosity in cast composite which was reduced by forging.

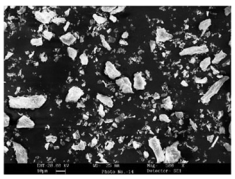

Fig. 1 – Shape and size of MnO_2 particles being used in Al-8Mg-MnO_2 composite synthesis.

The present study investigates the mechanical properties of cast Al-8Mg-MnO_2 composites synthesized by solidification of slurry of manganese oxide dispersed in molten aluminium-magnesium alloy, casted in water cooled copper mold for higher solidification rate. Al melt reduces the MnO_2 into Mn, and generates in-situ Al_2O_3. The sizes of the MnO_2 particles used here were in the range 1–20 μm but average size was almost constant in all the samples therefore the effect was similar in all samples. Moreover the effect of different particle size was not the objective of present study though many workers have reported effect of particle size on the mechanical properties of the composites. Sachit et al. [25] reported that mechanical properties increase with decrease in particle size. Whereas Kumar et al. [26] have observed that mechanical properties are superior in composites reinforced with coarse fly ash particles (103–150 μm) as compared to those of composites with fine particles (50–75 μm). However, J_{IC}, shows only a minor dependence on the size of the reinforcement [19]. Hamid et al. [12] reported that the MnO_2 particles in cast Al-Mg-MnO_2 composites had very good impact on mechanical properties. Therefore in this study an attempt is made to optimize content of MnO_2 at which best mechanical as well as fracture properties could be realized. In this study other parameters such as solidification rate, melt temperature, stirring duration, forging temperature and reduction are kept constant.

2. Experimental procedure

Commercial pure aluminum containing 99.60 pct Al, 0.202 pct Fe, 0.091 pct Si, and 0.102 pct Zn, as determined using an optical emission spectrometer (Thermo Jarrell Ash, Atom Comp 181), was used as matrix of the composite. Magnesium used for alloying purpose was 99.92 pct pure. The MnO_2 particles used for *in-situ* reaction with aluminum were of 5.02 gm/cm^3 density and 99.915% purity. It was supplied by Ranbaxy fine Chemicals Ltd, New Delhi, India. The sizes of the MnO_2 particles were in the range from 1 to 20 μm as shown in Fig. 1. Same powder mix was used in all the samples therefore it had same impact in all samples. The stirrer and MnO_2 particles were preheated to 400 °C before being used in order to prevent any significant decrease in temperature. It had also helped in removing the moisture content if any in the MnO_2 powder. Clay-graphite crucible was used to melt aluminum in a resistance heated muffle furnace and the temperature of molten aluminum was maintained at 800 °C. The temperature

Please cite this article in press as: Narain V, Ray S. Variation in mechanical properties with MnO_2 content in cast and forged in-situ Al-8Mg-MnO_2 composites. J Mater Res Technol. 2019. https://doi.org/10.1016/j.jmrt.2019.07.062

of the melt was measured by using a digital temperature indicator connected to a chromel-alumel thermocouple placed at 15–25 mm inside the melt. At this temperature, magnesium, wrapped in aluminium foil was added to the melt, which was thoroughly stirred for 2 min with the help of motor driven impeller at 700 rpm. A tachometer was used to measure the speed of the stirrer. MnO_2 particles were added slowly and continuously into Al-Mg melt by vibratory feeder and were mixed with the help of stirrer. The resulting slurry was maintained at 800 °C and stirred for 5 min before being cast into water cooled copper mold by bottom pouring mechanism. Three different composites were synthesized containing 3, 5 and 8 wt% of MnO_2 particles in Al-Mg melt having a fixed 8 wt% Mg in all the composites and these composites were designated as A8/3, A8/5 and A8/8 respectively. The cast ingots of composites were cut into two sections. One section was used for determining the properties of as-cast composites while the other section was hot forged at 400 °C to attain 22% reduction before being used for mechanical properties.

The chemical composition of the matrix alloy of *in-situ* composites had been analyzed by GBC AVANTA-M atomic absorption spectrometers (AAS). The Sample was prepared by dissolving 10 g of composite chips in 2 M hydrochloric acid (HCl) for selective dissolution of the aluminum alloy matrix without attacking unreacted MnO_2 and Al_2O_3 particles. Sodium sulfate (Na_2SO_4) was also added to settle down the suspended particles in the solution. The insoluble oxides were filtered out using ashless filter paper subsequently it was burnt completely in a pre-weighted silica crucible at 700 °C. The residue obtained was subjected to X-ray diffraction (XRD) analysis with a D8 Advance Brukes axs, Karlsruhe, Germany, X-ray diffractometer in the two theta range of 5°–110° using CuKα radiation target and nickel filter at a current of around 20 μA under a voltage of 35 KV. The filtered solution was analyzed by AAS to determine the amount of manganese and other elements in the matrix alloy.

The porosity of the composite was calculated with the help of density measurements. Density of the composite block (6 mm dia × 15 mm height) and the extracted particles were determined experimentally by water immersion method using ASTM C 135-96 standard. The volume of the cast in-situ composite,

$$V_c = V_m + V_o + V_p, \tag{2}$$

Where V_m, V_o and V_p were volume of the matrix alloy, oxides and voids, respectively. The mass of the composites was

$$W_c = W_m + W_o, \tag{3}$$

Where W_m was the mass of the matrix alloy, and W_o was the mass of the oxide particles produced in the melt. Therefore the density of the cast in-situ composites ρ_c may be written as

$$\rho_c = \frac{W_c}{V_c} = \frac{(W_m + W_o)}{(V_m + V_o + V_p)} \tag{4}$$

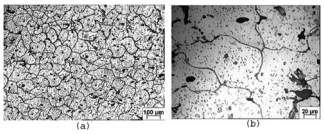

Fig. 2 – (a) Micrograph A8/8 composite etched with HF (b) Etched micrograph at higher magnification.

Or

$$V_p = \frac{(W_m + W_o)}{\rho_c} - \left(\frac{W_m}{\rho_m} + \frac{W_o}{\rho_o}\right) \tag{5}$$

Where ρ_C is the density of the in-situ composite which was determined by pycnometer method, ρ_m is the density of the matrix alloys, ρ_O is density of oxide formed in the composite. The oxide present in the composite was a mixture of oxides formed from direct oxidation of aluminum, oxidation of aluminum by MnO_2 particles, and unreacted MnO_2. Leaching of Al-8Mg alloy had provided content of Al_2O_3 formed from direct oxidation. Any increase in Al_2O_3 content in a composite sample, suggest the formation of alumina from MnO_2 particles.

Hardness test was carried out on 150 mm × 10 mm long rectangular bar using Brinell Hardness Tester. It was performed with a load of 31.625 kg for 10 s by a steel ball indenter of 2.5 mm diameter. The tensile tests of as cast and forged composites were conducted on cylindrical tensile specimens of gauge length 25 mm and diameter 5 mm at a constant displacement rate of 0.2 mm/min using universal testing machine (Hounsfield, Monsanto, H25KS/05, Surrey, England).

Fracture toughness tests were carried out on a servo hydraulic model 8800 Instron universal testing machine. Lab View, a programming environment application from National Instruments was used to get the interface between the program and the Instron Model 8800. Fracture toughness tests on C-T specimens of both as cast and forged composites were carried out following the standard ASTM E813-81. The specimen was pre-fatigued before measuring load–load line displacement with the help of clip-gage in order to arrive at *J-R* curve for the composites using single specimen. The crack lengths at different loads were estimated from compliance by loading-unloading at different J-values. The blunting lines were drawn at 0.2 mm offset following the equation,

$$J = 2M\sigma_f \Delta a \tag{6}$$

Where M = 1, flow stress σ_f was arithmetic mean of yield strength and tensile strength and Δa was the crack extension. The program determines the exact point of intersection of *J-R* curve with blunting line. Plane strain condition was verified by the following equation.

$$B.b > 2.5J_{IC}/\sigma_f \tag{7}$$

Where B is the specimen thickness, b is the uncracked ligament length and σ_f is the effective flow strength. All the tests conducted in this study satisfied this criterion and the slopes of the *J-R* curves were also positive. The crack propagation behaviour was characterized by the tearing modulus concept.

Please cite this article in press as: Narain V, Ray S. Variation in mechanical properties with MnO_2 content in cast and forged in-situ Al-8Mg-MnO_2 composites. J Mater Res Technol. 2019. https://doi.org/10.1016/j.jmrt.2019.07.062

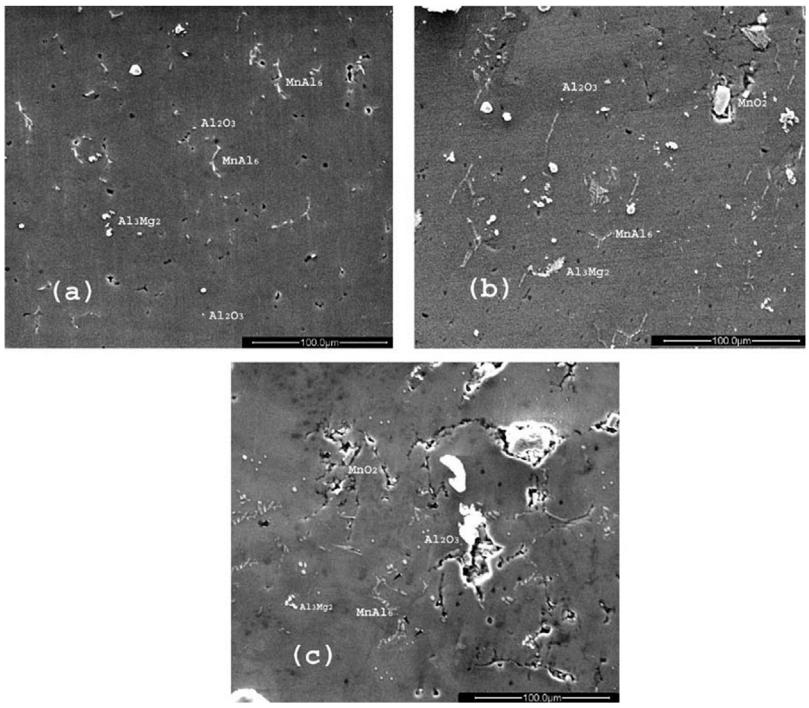

Fig. 3 – Unetched SEM micrograph of A8/3 Composite. (b) Unetched SEM micrograph of A8/5 Composite. (c) Unetched SEM micrograph of A8/8 Composite.

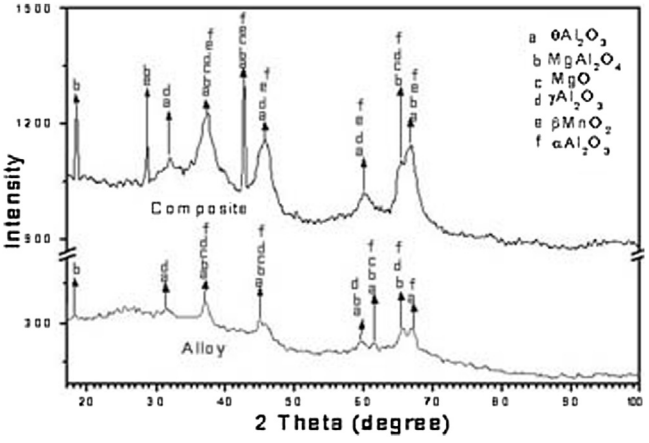

Fig. 4 – Comparison of XRD pattern of particles extracted from Al-8Mg-MnO_2 composite and the Al-Mg alloy.

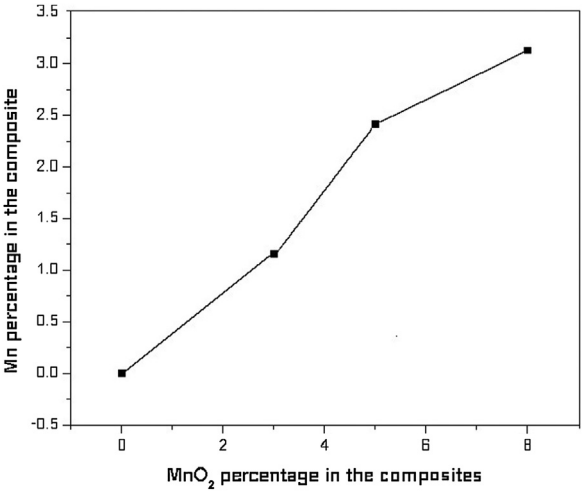

Fig. 5 – Variation of Mn in the Al-8Mg-MnO_2 composite with increasing MnO_2 content.

3. Result and discussion

The optical microstructure of a typical as cast composite is shown in Fig. 2 at relatively lower and higher magnification. The microstructure of the composite in Fig. 2(a) reveals the grain structure of the matrix alloy which has well distributed dark particles. The precipitates at dendrite boundaries are shown at higher magnification in Fig. 2(b). Fig. 3(a–c) shows a typical unetched micrograph of *in-situ* Al-8Mg-MnO_2 composites, containing 3, 5, and 8 wt% of MnO_2 respectively. Addition of 8 wt% Mg into the aluminium melt forms intermetallic Al_3Mg_2 and oxides of Al and Mg, which are visible in all the three micrographs. The oxides formed in the alloy were due to direct oxidation of the Al and Mg. On addition of MnO_2, in-situ reduction of manganese dioxide by molten aluminum had released Mn and Al_2O_3 into the melt. An intermetallic phase, $MnAl_6$, was formed due to the release of manganese beyond its solid solubility limit. As the percentage of MnO_2 was increased, there was an increase in the amount of Al_2O_3, and $MnAl_6$ as is evident from the Fig. 3(a–c). Fine $MnAl_6$ were precipitated along the grain boundary as clearly suggested in the micrograph. The alumina formed in the composite is either due to oxidation of aluminum melt by MnO_2 particles through the following chemical reaction

$$MnO_2 + Al = Mn + Al_2O_3, \quad (8)$$

Please cite this article in press as: Narain V, Ray S. Variation in mechanical properties with MnO_2 content in cast and forged in-situ Al-8Mg-MnO_2 composites. J Mater Res Technol. 2019. https://doi.org/10.1016/j.jmrt.2019.07.062

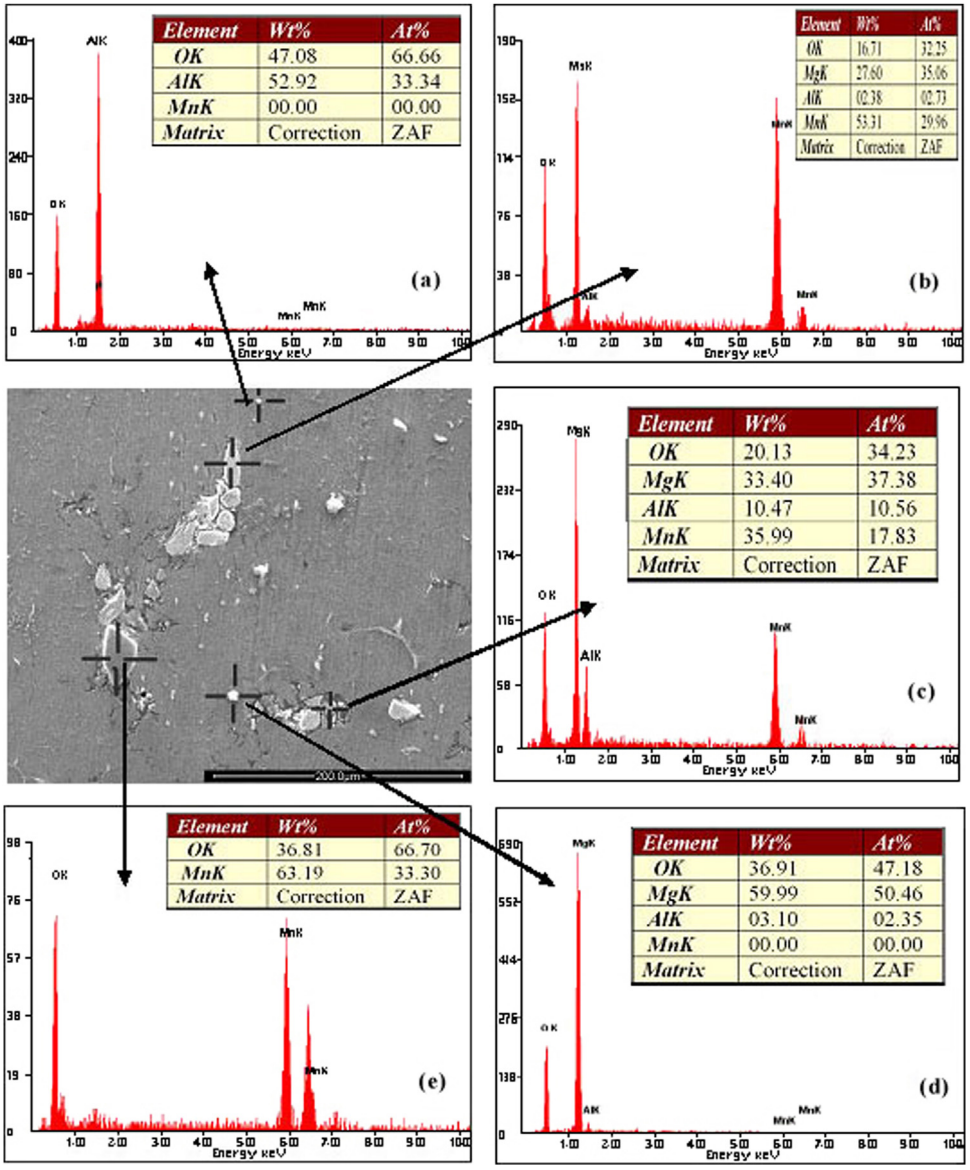

Fig. 6 – EDS analysis of Al-8Mg-MnO_2 based composites (a) Al oxide (b) & (c) Al-Mg-Mn oxide (d) Mg-Oxide (e) MnO_2.

or by direct oxidation of aluminium melt during heating. Alumina formed during in-situ reaction is very fine and mostly circular in nature. The direct oxidation of aluminium also happens at the time of Al-Mg alloy formation. Therefore to know whether alumina formed was due to in-situ reaction or direct oxidation, XRD patterns of Al-Mg alloy and Al-8Mg-MnO_2 composite were compared. An increase in the alumina content in XRD pattern of composite would suggest that extra alumina came through in-situ reaction in which Mn and alumina were released into the melt.

The XRD pattern of the extracted particles obtained after leaching the matrix alloy and the Al-8Mg-MnO_2 composites is shown in Fig. 4. Since the peaks are fairly broad, this may indicate small size of crystallites and overlapping of peaks from many compounds. The peaks indicate the presence of the following phases: γAl_2O_3, θAl_2O_3, αAl_2O_3, βMnO_2, $MgAl_2O_4$, and MgO. But there is no independent peak from either of

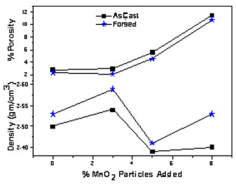

Fig. 7 – Variation of porosity and density with increasing addition of MnO_2 in Al-8Mg- MnO_2 composite.

γAl_2O_3, θAl_2O_3 or αAl_2O_3. Fig. 4 also shows XRD pattern of the extracted particles obtained after leaching of Al-Mg base alloy. Comparison of both the patterns suggests that MnO_2 particles added to the composite had contributed significantly towards the existence $MgAl_2O_4$, MgO and Al_2O_3 apart from unreacted MnO_2. The intermetallic $MnAl_6$ did not appear in the XRD pattern. This may be due to dissolution of $MnAl_6$ during acid

Please cite this article in press as: Narain V, Ray S. Variation in mechanical properties with MnO_2 content in cast and forged in-situ Al-8Mg-MnO_2 composites. J Mater Res Technol. 2019. https://doi.org/10.1016/j.jmrt.2019.07.062

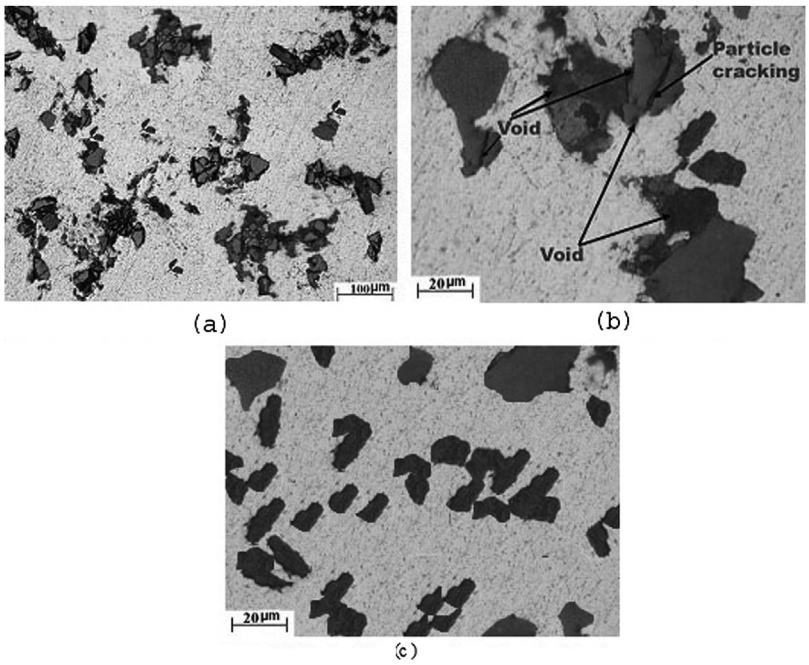

Fig. 8 – (a) MnO_2 particles distribution in forged composite (b) Particle cracking after forging. (c) De-clustering of MnO_2 particles after forging.

Table 1 – Density and porosity in cast and forged alloys and composites.

Sample	Density (gm/cm^3)		Porosity %	
	Cast	Forged	Cast	Forged
A8/0	2.50	2.53	2.74	2.33
A8/3	2.54	2.59	2.88	2.05
A8/5	2.44	2.46	5.50	4.48
A8/8	2.45	2.53	11.48	10.70

leaching for particle extraction. Manganese released in the composite due to in-situ reaction was measured with the help of AAS. Manganese content in the composites synthesized by additions of 3, 5, and 8 wt% MnO_2 shows 1.134%, 2.414% and 3.128 wt% manganese in the respective composites. Variation of manganese content with MnO_2 content is shown in Fig. 5.

EDX analysis in Fig. 6 shows formation of an intermetallic product containing Al, Mg and Mn. The particle analyzed in Fig. 6(a) is that of alumina. Fig. 6(b) and (c) shows oxides of Al-Mg-Mn, Fig. 6(d) shows MgO and Fig. 6(e) shows MnO_2 particles in the composite which were added externally. The suggestions made by EDX analysis are also supported by XRD pattern.

The variation of porosity and density, with increased amount of MnO_2 particles is shown in Fig. 7. It does not show any consistent trend in density variation with increased amount of MnO_2 particles, but porosity increases considerably with increased MnO_2 particles.

The impact of forging on microstructures is shown in Fig. 8. It shows that at certain locations more particles are clustered possibly due to flow of softer matrix residing between particle rich regions, as visible in Fig. 8(a). Forging

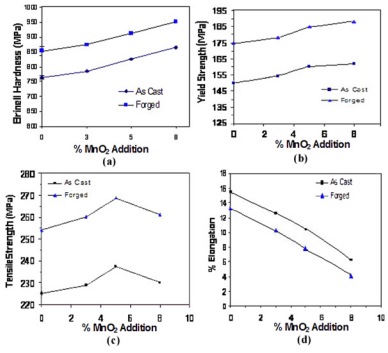

Fig. 9 – Variation of mechanical Properties of as cast and forged Al-8Mg-MnO_2 composites with MnO_2 content: (a) Hardness, (b) Yield strength, (c) Tensile strength and (d) Percentage elongation.

has also caused particle cracking, and voids formation within the cluster as observed in Fig. 8(b). Apart from the above impact at certain location, forging has very positive impact in separating out clustered particles and eliminated debonding at particles-matrix interface as observed Fig. 8(c). It has enhanced mechanical properties of the composite.

Mechanical properties of the cast and forged composite are shown in Fig. 9. Fig. 9(a) shows significant increase in hardness of the composite after forging, as the percentage of MnO_2 is increased from 3 to 8 wt%. This may be due to the work hardening of the matrix as well as healing of porosity formed during casting (Table 1). The variations of yield strength, tensile strength and ductility in terms of percent elongation with increasing particle content in both the

Please cite this article in press as: Narain V, Ray S. Variation in mechanical properties with MnO_2 content in cast and forged in-situ Al-8Mg-MnO_2 composites. J Mater Res Technol. 2019. https://doi.org/10.1016/j.jmrt.2019.07.062

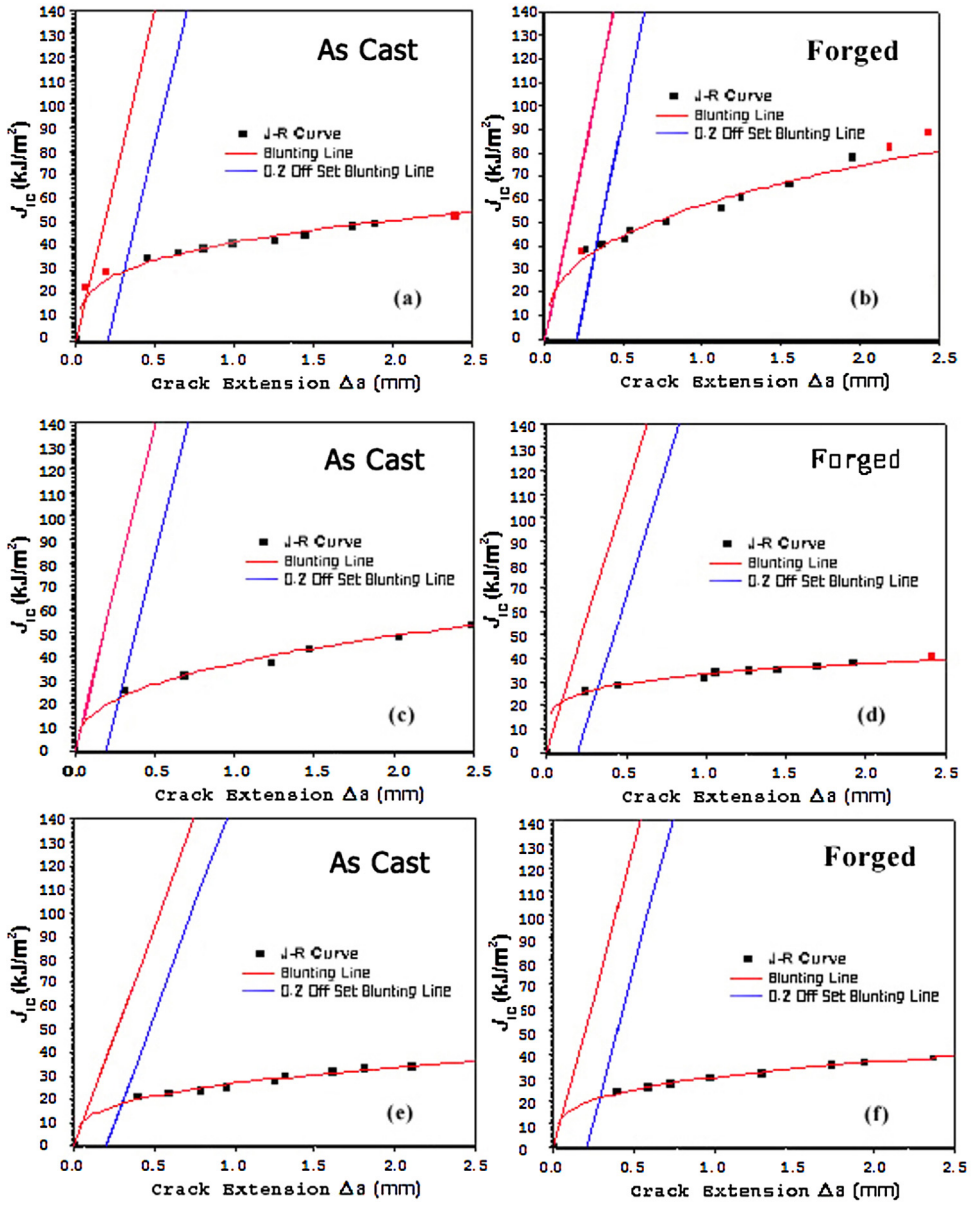

Fig. 10 – J–R curves of as cast and forged Al-8Mg-MnO_2 composites with different particle contents: (a) cast A8/3, (b) forged A8/3, (c) cast A8/5 (d) forged A8/5 (e) cast A8/8 and (f) forged A8/8.

forged and cast composites are shown in Figs. 9(b), (c) and (d) respectively. In cast composites, yield strength increases and ductility decreases with increased amount of MnO_2 particles as observed by earlier workers [12,18], presumably due to restraint on the deformation of matrix imposed by the presence of particles. Tensile strength in cast composites increases significantly and reaches to its peak when particle content increased from 3 to 5 wt% but further increase in particle content to 8 wt% decreases tensile strength significantly. This may be attributed due to enhanced porosity (Table 1), which has reduced the effective cross-sectional area and so the tensile strength. After forging, there is significant increase in yield and tensile strength but trend of increase in yield and tensile strengths are similar as of cast composite. With increasing MnO_2 content there is decrease in percentage elongation. Forging has decreased further, as shown in Fig. 9(d).This may be because forging was not able to heal the porosity in great extent, and particle clusters in the matrix were opened up resulting in voids (Fig. 8(b)) and deteriorated the mechanical properties as also been reported by Balasubramaniam et al [23].

The *J*-*R* curves of as cast and forged composites containing 3, 5 and 8 wt% oxide particles, designated as A8/3, A8/5 and A8/8, are shown in Fig. 10(a)–(f). The initiation of fracture does not take place simultaneously across the entire crack front. An offset of 0.2 mm is taken to draw the blunting line and its intersection with *J*-*R* curve indicates the initiation fracture toughness, J_{IC}. Initiation fracture toughness, J_{IC}, of cast composites, determined either by the blunting line without offset or with offset blunting line, decreases with increasing particle

Please cite this article in press as: Narain V, Ray S. Variation in mechanical properties with MnO_2 content in cast and forged in-situ Al-8Mg-MnO_2 composites. J Mater Res Technol. 2019. https://doi.org/10.1016/j.jmrt.2019.07.062

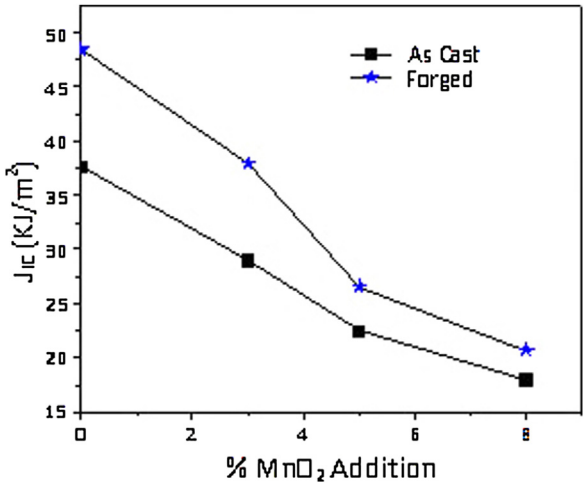

Fig. 11 – Variation of fracture toughness, J_{IC} of as cast and forged Al-8Mg-MnO_2 composites with MnO_2 content.

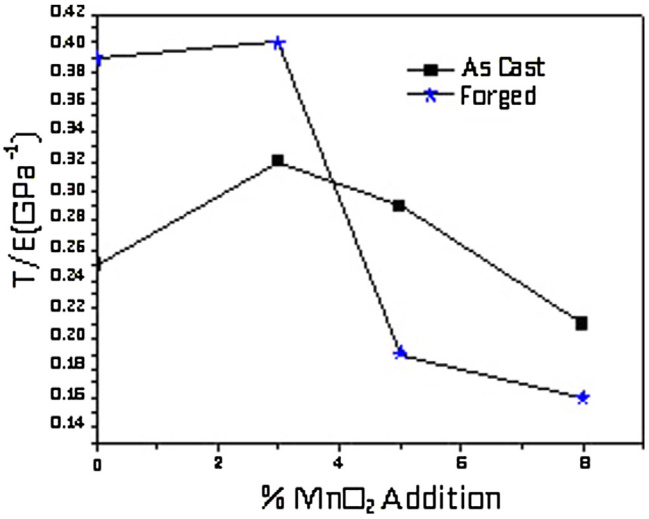

Fig. 12 – Variation of T/E for as cast and forged Al-8Mg-MnO_2 composites with different MnO_2 contents.

content as shown in Fig. 11. On forging, there is increase in the J_{IC} of composites as similar to that reported by Pillai et al. [22]. This increase is more prominent in low content MnO_2 composites but J_{IC} decreases continuously with increasing MnO_2 content as is observed in cast composites.

The ratio of tearing modulus to elastic modulus, which depends on the slope of the *J*-*R* curve and flow stress, is higher in as cast composites compared to that in forged composites. But an interesting result has been observed in forged 3 wt% MnO_2 composite where growth toughness is higher than that in cast composite and a sudden drop is observed when MnO_2 content increases from 3 to 5 and 8 wt% and even these values are lower than those in the cast composites. T/ E ratio is the ratio of slope of *J*-*R* curve and the square of the flow stress. Forging has increased the flow stress in all the cases but inverse of square of the flow stress of forged and cast composites have very little difference. Therefore the slope of *J*-*R* curve is the dominating factor to decide the value of T/E ratio. At 3 wt% MnO_2, slope of forged composite was more than that of the cast composite therefore T/E ratio is more. In case of 5 wt%MnO_2 there is a sharp decrease in the slope of *J*-*R* curve for the forged composite. Due to this reason there is a sharp decrease in T/E ratio for forged composite in comparison to that in cast composite. Slope of *J*-*R* curve is the rate of change of *J* with respect to crack extension. At 3 wt% MnO_2, forging has healed the pores and made the crack extension difficult, which produces higher slope for forged composite. In case of 5 wt% MnO_2, instead of healing of voids, forging has increased void at particle matrix interface and cracking of particles. It has facilitated easy path for crack extension with respect to the cast composite. Due to this reason there is a sudden drop in T/E ratio value for forged composite in comparison to that in cast composite. In cast composite, T/E ratio decreases with increased particle content because of dominating influence of increased flow stress over the increased slope of the *J*-*R* curve as shown in Fig. 12. The increased MnO_2 addition to 8 wt% in cast composites shows a slight decrease in flow stress and the slope of *J*-*R* curve, which produces drastic reduction in T/E ratio.

4. Summary and conclusions

Cast composites A8/3, A8/5 and A8/8 synthesized by dispersion of 3, 5 and 8 wt% of MnO_2 particles in molten Al-8 wt% Mg alloy and after forging have led us to the following conclusions.

1 The microstructure of the composite shows precipitates of intermetallic containing Al, Mg and Mn at dendrite boundaries and alumina particles which are formed by the reduction of MnO_2 particles in molten Al-Mg alloy.
2 The hardness, yield and tensile strength of as cast composites increase with increasing MnO_2 addition. It may be due to increasing presence of oxide particles, reduced grain size and enhanced released manganese. Tensile strength increases with increasing MnO_2 addition till 5 wt%. A higher addition of 8 wt% MnO_2 decreases the tensile strength due to increased clustering, and early void formation. Forging has increased hardness, yield and tensile strength further due to reduction in porosity and work hardening.
3 The ductility of the cast composites decreases with increasing addition of MnO_2 particles in the composites, which may be due to increased clustering and higher release of manganese. It has an embrittling influence on the matrix Al-Mg alloy. Forging decreases the ductility in comparison to corresponding cast composites, which may be attributed to fracture of reinforcement particles and their debonding during forging. It leads to early void nucleation during plastic straining. However, the variation of ductility with increasing addition of MnO_2 in the composites is similar to that observed in cast composites.
4 The initiation fracture toughness, J_{IC} decreases as MnO_2 particle content increases in the composite from 3 to 8 wt%. After forging there is an improvement in J_{IC} of the composites. This improvement is more in low MnO_2 based composite.
5 The T/E ratio in cast composite decreases with increasing particle content because of dominating influence of

Please cite this article in press as: Narain V, Ray S. Variation in mechanical properties with MnO_2 content in cast and forged in-situ Al-8Mg-MnO_2 composites. J Mater Res Technol. 2019. https://doi.org/10.1016/j.jmrt.2019.07.062

increased flow stress over the increase in slope of the *J*-*R* curve. The composites of 3 wt% MnO_2 could give significant advantage in growth toughness without impairing initiation fracture toughness over that of the alloy. Increase in particle addition beyond 3 wt% MnO_2 decreases rapidly both the initiation fracture toughness and the growth toughness, which may be attributed to increased brittleness due to clustering and the increased alloying of the matrix by manganese.

Conflicts of interest

The authors declare no conflicts of interest.

REFERENCES

[1] Ray S. Casting of metal matrix composites. In: Newaz GM, Neber-Aeschbacher H, Wohlbier FH, editors. Metal matrix composites, Part 1: applications and processing. Trans Tech Publications; 1995. p. 417–46.
[2] Allison JE, Cole GS. Metal-matrix composites in the automotive industry: opportunities and challenges. JOM 1993;45(1):19–25.
[3] Maity PC, Panigrahi SC, Chakraborty PN. Preparation of aluminium-alumina in-situ particle composite by addition of titania to aluminium melt. Scripta Metall Mater 1993;28:549–52.
[4] Maity PC, Chakraborty PN. Preparation of Al-MgA1_2O_4-MgO in situ particle-composites by addition of MnO_2, particles to molten Al-2 wt% Mg alloys. Mater Lett 1994;20:93–7.
[5] Yoshikawa N, Watanabe Y, Veloza ZM, Kikuchi A, Taniguchi S. Microstructure-process-Property realationship in Al/Al_2O_3 composites fabricated by reaction between SiO_2 and molten Al. Key Eng Mater 1999;161–163:311–4.
[6] Fan T, Zhang D, Yang G, Shibayanagi T, Naka M. Fabrication of in situ Al_2O_3/Al composite via remelting. J Mater Proc Technol 2003;142:556–61.
[7] Maity PC, Chakraborty PN, Panigrahi SC. Al-Al_2O_3 in situ particle composites by reaction of CuO particles in molten pure Al. Mater Lett 1997;30:147–51.
[8] Geng K, Lu W, Zhang D. In situ synthesized (TiB + Y_2O_3)/Ti composites. J Mater Sci Lett 2003;22:877–9.
[9] Li YF, Qin CD, Ng DHL. Morphology and growth mechanism of alumina whiskers in aluminum-based metal matrix composites. J Mater Res 1999;44:2997–3000.
[10] Yu P, Deng C-J, Ma N-G, Dickon HL. Ng: a new method of producing uniformly distributed alumina particles in Al-based metal matrix composite. Mater Lett 2004;58:679–82.
[11] Subramanian R, McKamey CG, Schneibel JH, Buck LR, Menchhofer PA. Iron aluminide–Al_2O_3 composites by in situ displacement reactions: processing and mechanical properties. Mater Sci Eng A Struct Mater Prop Microstruct Process 1998;254:119–23.
[12] Hamid Abdulhaqq A, Ghosh PK, Jain SC, Ray S. Processing Microstructure and mechanical properties of cast in-situ Al(Mg, Mn)-Al_2O_3(MnO_2) composite. Metall Mater Trans A 2005;36A:2211–23.
[13] Shabestari SG, Moemeni H. Effect of copper and solidification conditions on the microstructure and mechanical properties of Al-Si-Mg, alloys. J Mater Process Technol 2004;153:193–8.
[14] Caceres CH, Davidson CJ, Griffiths JR. The deformation and fracture behaviour of an Al-Si-Mg casting alloy. Mater Sci Eng 1995;197:171–9.
[15] Wang QG. Microstructural effects on the tensile and fracture behavior of Aluminum casting alloys A356/357. Metall Mater Trans 2003;34:2887–99.
[16] Mae H, Teng X, Bai Y, Wierzbicki T. Comparison of ductile fracture properties of aluminum castings: sand mold vs. Metal mold. Int J Solids Struct 2008;45:1430–44.
[17] Zhang S-L, Zhao Y-T, Chen G, Cheng X-N, Dai Q-X. Microstructures and mechanical properties of aluminum matrix composites fabricated from Al–x wt.% Zr(CO_3)2 (x = 5, 10, 15, 20, 25) systems. J Alloys Compd 2007;429:198–203.
[18] Xing ZP, Guo JT, Han YF, Yu LG. Microstructure and mechanical behavior of the NiAl–TiC in-situ composite. Metall Trans A 1997;28A(4):1079–87.
[19] Manoharan M, Lewandowski JJ. Effect of reinforcement size and matrix microstructure on the fracture properties of an aluminum metal matrix composite. Mater Sci Eng 1992;A150:179–86.
[20] Manoharan M, Lewandowski JJ. Crack initiation and growth toughness of an aluminum metal matrix composite. Acta Metall Mater 1990;38(3):489–96.
[21] Umit Cocen and Kazim Onel. Ductility and strength of extruded SiC_p/aluminium-alloy composites. Compos Sci Technol 2002;62:275–82.
[22] Pillai UTS, Pandey RK, Rohatgi PK. Effect of volume fraction and size of graphite particulates on fracture behaviour of AL-graphite composites. Eng Fract Mech 1987;28(4):461–77.
[23] Balasubramanian PK, Srinivasa RP, Sivadasan KG, Sathyanarayana KG, Pai BC, Rohatgi PK. Forging characteristics of Al-Zn-Mg alloy containing 5 wt% TiO_2 dispersion. J Mater Sci Lett 1989;8:799–801.
[24] Ghanaraja S, Ray S, Nath SK. Comparative study of tensile properties of cast and hot forged alumina nanoparticle reinforced composites. Int J Mater Metall Eng 2016;10(6):688–95.
[25] Sachit TS, Sapthagiri PN, MohammedAameer K. Effect of particle size on mechanical and tribological behavior of LM4/SiCp based MMC. Mater Today Proc 2018;5(2):5901–7. Part 1.
[26] Ravi KK, Mylsamy MK, Ganesan A, Ramanathan S. Effect of particle size on mechanical properties and tribological behaviour of aluminium/fly ash composites. Sci Eng Compos Mater 2012;19(3):247–53.

Please cite this article in press as: Narain V, Ray S. Variation in mechanical properties with MnO_2 content in cast and forged in-situ Al-8Mg-MnO_2 composites. J Mater Res Technol. 2019. https://doi.org/10.1016/j.jmrt.2019.07.062